J Solid State Electrochem (2003) 7: 678–683
DOI 10.1007/s10008-003-0370-3

ORIGINAL PAPER

Bing-Joe Hwang · Raman Santhanam
Chung-Ru Wu · Yin-Wen Tsai

Nucleation and growth mechanism for the electropolymerization of aniline in trifluoroacetic acid/lithium perchlorate/propylene carbonate medium

Received: 13 November 2002 / Accepted: 14 February 2003 / Published online: 4 April 2003

Abstract In the present work, the nucleation and growth mechanism for the electropolymerization of aniline in propylene carbonate medium containing 0.06 M trifluoroacetic acid and 0.05 M lithium perchlorate was investigated at different potentials on highly oriented pyrolytic graphite (HOPG) by potentiostatic current-time transients (*i-t*) and atomic force microscopic (AFM) measurements. The electrochemical data fitted with the theoretical curves for nucleation and growth suggest that the electropolymerization of aniline consists of progressive nucleation followed by 3D growth at an early stage and layer-by-layer growth in subsequent periods. The results obtained from transient analysis were in good agreement with the results of the AFM analysis. In our previous studies with aqueous solutions, we observed only progressive nucleation followed by a 3D growth mechanism for the electropolymerization of aniline in a higher potential range, 1.5–2.0 V vs. Ag/AgCl. Hence, the results obtained from the present work indicate that the nucleation and growth mechanism depends on the medium.

Keywords Atomic force microscopy · Layer-by-layer model · Nucleation and growth · Polyaniline

Introduction

In recent years, the deposition of conducting polymer films on electrode surfaces has attracted great attention because of their wide range of applications in batteries, capacitors, ion sensors and electrochromic devices [1, 2, 3, 4, 5, 6, 7]. The electrochemical properties of polymers mainly depend on surface properties. It is essential, therefore, to understand the microstructure of polymers under various conditions for the development of future applications.

Mostly, nucleation and growth mechanisms of conducting polymers have been studied in aqueous media [8, 9, 10, 11, 12, 13, 14, 15, 16, 17]. In particular, however, nucleation and growth mechanisms of polythiophene and its derivatives have been carried out in non-aqueous media [18, 19, 20]. In all these studies, mostly the predictions of the nucleation and growth mechanism have been made only by current-time transient measurements. However, for better understanding, it is important to verify the mechanism by some other suitable technique. In this point of view, atomic force microscopy (AFM) has been found to be an effective technique to examine the surface morphology of the conducting polymers [21, 22].

In recent papers, we reported the nucleation and growth mechanism for the electropolymerization of polypyrrole [22, 23] and polyaniline [24, 25] in aqueous media. In this paper we report the nucleation and growth mechanism of polyaniline in non-aqueous media at different anodic potentials and the mechanism is found to be different from that in aqueous media. This indicates that the nucleation and growth mechanism is strongly dependent on the medium. A mechanism is proposed from current-time transient measurements and compared with theoretical models. The proposed mechanism is also verified by AFM images.

B.-J. Hwang (✉) · R. Santhanam · C.-R. Wu · Y.-W. Tsai
Microelectrochemistry Laboratory,
Department of Chemical Engineering,
National Taiwan University of Science and Technology,
43 Keelung Road, sec. 4, 106 Taipei,
Taiwan, Republic of China
E-mail: bjh@ch.ntust.edu.tw
Tel.: +886-2-27376624
Fax: +886-2-27376644

Experimental

The electrochemical polymerization of aniline was carried out by a potentiostatic method at 0.8–1.5 V, using a standard three-electrode cell. The highly oriented pyrolytic graphite (HOPG) working electrode used in this investigation has a surface area of 0.2375 cm^2 and was cleaved before use. Platinum/titanium mesh and saturated calomel electrodes were used as counter and reference electrodes, respectively. The concentration of aniline was 0.04 M in all the

experiments throughout the study. Propylene carbonate containing 0.06 M trifluoroacetic acid and 0.05 M lithium perchlorate was used as a supporting electrolyte solution. Before each experiment the supporting electrolyte was purged with nitrogen for about 30 min. Chronoamperometric measurements during anodic electrodeposition of polyaniline were controlled via a potentiostat (model 273A, EG&G, Princeton Applied Research) and recorded on a computer. The morphology of the polyaniline films deposited on HOPG was observed with a tapping mode atomic force microscope (Digital Instruments, Nanoscope III, 125 μm AFM scanning head). The material of the AFM cantilevers (Digital Instruments) was an edged single crystal of n-type silicon. The tip has a shape with a 10 nm radius of curvature and 35° interior angle. Images were captured at a rate of 0.25 frame/min. During AFM measurements, considerable searching was done to find images on various parts of the film and here we show the images that we could find in several parts on the film. Most of the areas examined produced reproducible images similar to those shown in this paper.

Results and discussion

Figure 1 shows typical current-time transient curves for formation of a polyaniline layer obtained at different potentials in the range 0.8–1.5 V vs. SCE in 0.04 M aniline/0.06 M CF_3COOH/0.05 M $LiClO_4$ in propylene carbonate medium on HOPG substrate. In this figure, the value of the current maximum, I_{max}, increases with the increase of potential. The shape of the current plateau after I_{max} is the characteristic feature of layer-by-layer growth of polyaniline nuclei [26]. The I_{max} values can be analyzed by comparing the experimental data with the theoretical curves given for the different types of nucleation and growth processes [5]. A comparative evaluation of experimental data with the theoretical curves of instantaneous/progressive nucleation followed by 2D and 3D growth, under diffusion control, is shown in Figs. 2 and 3 respectively. As seen in Fig. 2, the experimental data deviate significantly from theoretical curves for 2D instantaneous/progressive nucleation. Then, a comparison of experimental data with the theoretical curves for instantaneous/progressive 3D indicates that the nucleation and growth mechanism is in between instantaneous 3D and progressive 3D before I_{max}. Both 2D and 3D models failed to fit with the experimental data after I_{max}. Then, a schematic representation of various nucleations with the theoretical curves for instantaneous/progressive 3D nucleation and growth is shown in Fig. 4. It seems that the nucleation follows progressive 3D before I_{max} and after that a layer-by-layer model is appropriate.

A model for layer-by-layer growth may be developed by considering the equations developed for 3D progressive nucleation and growth [5]. The current generated for 3D progressive nucleation is given by:

$$i_0 = X\left[1 - \exp\left(-Yt^2\right)\right] \quad (1)$$

where $X = zFD^{1/2}C/\tau^{1/2}t1^{/2}$ and $Y = AN\infty\tau k'D/2$, with F = molar charge of the depositing species, D = diffusion coefficient of the depositing species, C = bulk concentration, t = time, A = steady-state nucleation rate constant per site, N_∞ = maximum number of nuclei obtainable under prevailing conditions, and k' = a numerical constant determined by the conditions of the experiment.

The layer-by-layer growth can also be attempted in a similar manner to single layer growth. Consider a patch of first new nuclei generated on the surface of the old nuclei at time τ_1 which will generate a current, i_1, due to the succeeding layer at time t. Then the current, i_1, can be written as:

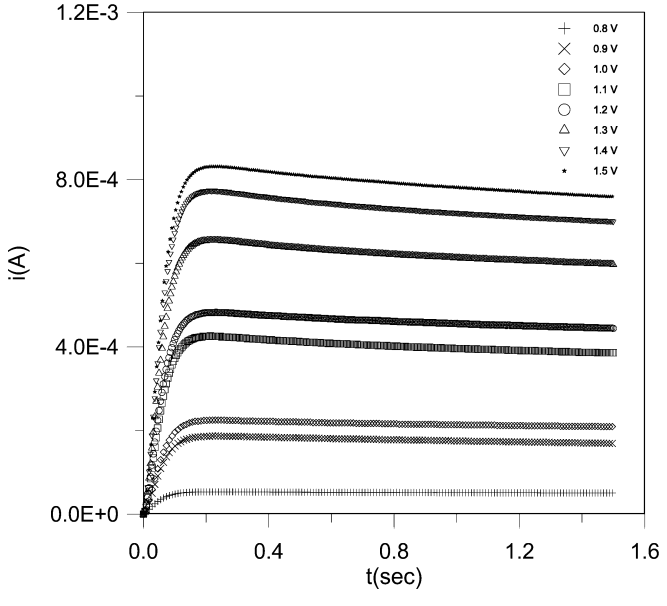

Fig. 1 The *i-t* transients for electropolymerization of aniline in 0.04 M aniline/0.06 M CF_3COOH/0.05 M $LiClO_4$ in propylene carbonate medium on HOPG at different potentials

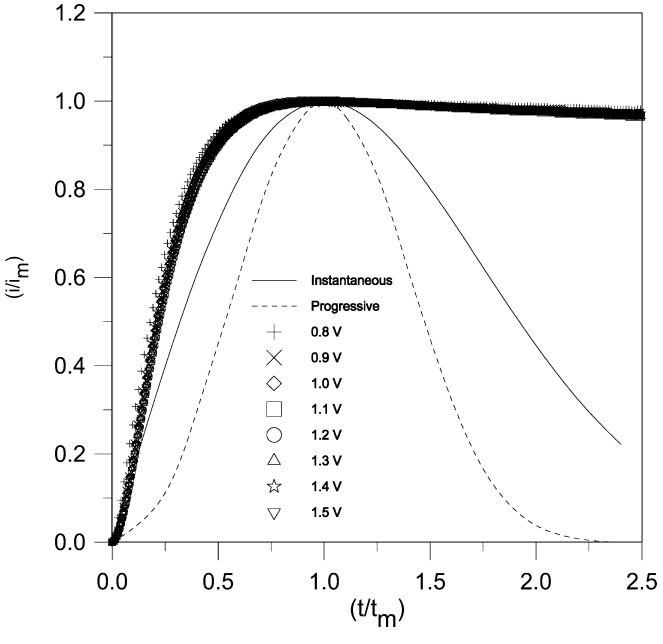

Fig. 2 Dimensionless plot of current maxima shown in Fig. 1 compared with theoretical curves for 2D instantaneous and progressive nucleation

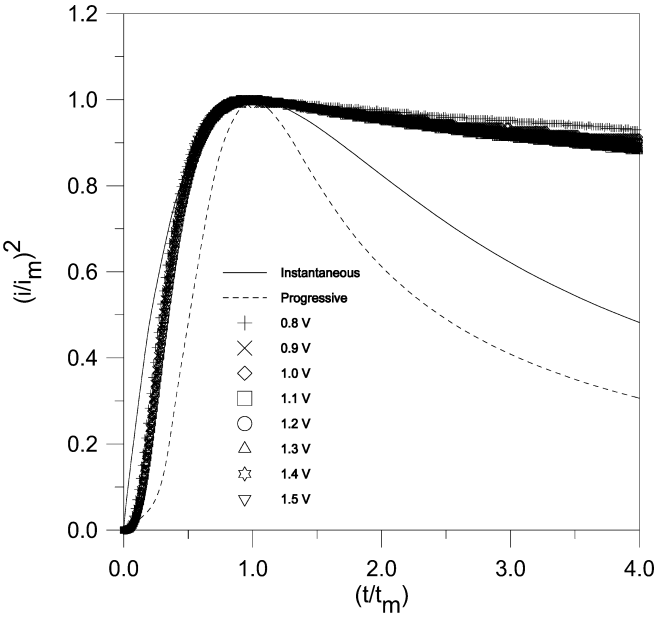

Fig. 3 Dimensionless plot of current maxima shown in Fig. 1 compared with theoretical curves for 3D instantaneous and progressive nucleation

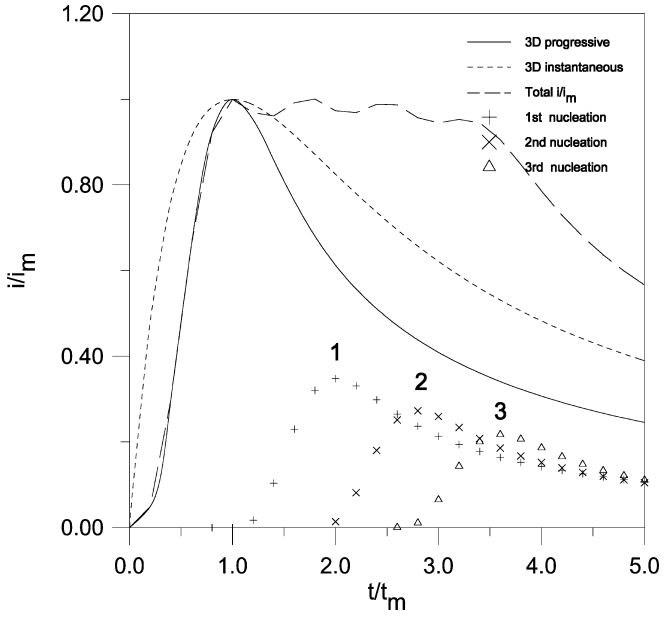

Fig. 4 Schematic representation of layer-by-layer growth. The first, second and third nucleations are indicated by corresponding numbers

$$i_1 = X[1 - \exp\{-Y(t-\tau_1)2\}]U(t-\tau_1) \quad (2)$$

For a patch of second nuclei generated at time τ_2:

$$i_2 = X\left[1 - \exp\left\{-Y(t-\tau_2)^2\right\}\right]U(t-\tau_2) \quad (3)$$

For a patch of third nuclei generated at time τ_3:

$$i_3 = X\left[1 - \exp\left\{-Y(t-\tau_3)^2\right\}\right]U(t-\tau_3) \quad (4)$$

Hence, the total current:

$$i = i_0 + i_1 + i_2 + i_3 + \ldots \quad (5)$$

is given by:

$$i = X\left(\begin{array}{l}\left[1 - \exp\left(-Yt^2\right)\right]U(t-\tau_0) + \left[1 - \exp\left\{-Y(t-\tau_1)^2\right\}\right]U(t-\tau_1) + \left[1 - \exp\left\{-Y(t-\tau_2)^2\right\}\right]\times \\ U(t-\tau_2) + \left[1 - \exp\left\{-Y(t-\tau_3)^2\right\}\right]U(t-\tau_3) + \ldots\end{array}\right) \quad (6)$$

where $\tau_0 = 0$, then:

$$i = X\left[\sum_{i=0}^{\infty}\left\{1 - \exp\left(-Y(t-\tau_i)^2\right)\right\}U(t-\tau_i)\right] \quad (7)$$

Thus:

$$i = X\left[\sum_{i=0}^{\infty}U(t-\tau_i) - \sum\exp\left(Y(t-\tau_i)^2\right)U(t-\tau_i)\right] \quad (8)$$

where U is the unit step function. It is difficult to determine the time delay, τ_i, because it depends on the electrode substrate, the potential and the concentration of the electrolyte. The I_{max} values for the first nucleation, second nucleation, third nucleation, etc., decrease due to the development of a diffusive layer. A schematic representation of the first, second and third nuclei generation is presented in Fig. 5.

One can furnish a possible explanation for the deviation of experimental data with the theoretical curves in Fig. 3. In this figure, the experimental data follow a progressive 3D mechanism in the initial stage of the nucleation and growth and then deviate from a 3D progressive mechanism. This is possible when $\tau < t_{max}$. Hence it may be stated that the layer-by-layer growth started forming before I_{max} itself. In the schematic representation (Fig. 4), the nucleation and growth mechanism follows well with progressive 3D before I_{max}. This is possible only when $\tau > t_{max}$ (from Fig. 3 it can be concluded that $\tau < t_{max}$).

In order to verify the nucleation and growth mechanism, obtained from potentiostatic current-time transient measurements, for the electropolymerization of aniline, another effective surface analytical tool is essential. Here AFM is used effectively to observe the mechanism of nucleation and growth of polyaniline. Figure 6a and Fig. 6b show the 2D and 3D views of AFM images obtained for the electropolymerization of aniline at 1.4 V in 0.04 M aniline/0.06 M CF_3COOH/0.05 M $LiClO_4$ in propylene carbonate medium on a HOPG substrate, respectively. The polymerization time is 0.025 s. As can be seen in Fig. 6b, the polyaniline

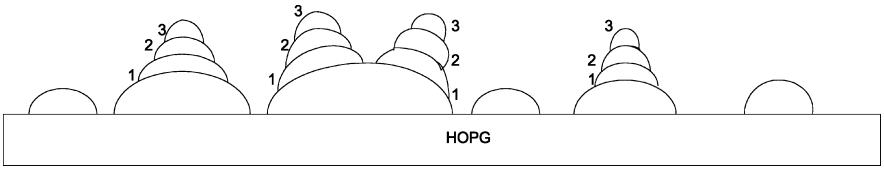

Fig. 5 Schematic representation of first, second and third nuclei formation

nuclei grow on their former positions and also on some new nuclei, especially in the center portion of the image, which form smaller nuclei particles where the surface morphology is flatter. Moreover, the growth rate of all nuclei is essentially equal and comparable on parallel and perpendicular directions to the electrode surface. These features strongly support the progressive 3D nucleation and growth of polyaniline nuclei in propylene carbonate medium on a HOPG substrate surface at an early stage.

Then the polymerization time was increased to 0.05 s. The features of the images are similar to the images obtained after 0.025 s. Both 2D and 3D views of these images are shown in Fig. 7. When the polymerization time is increased above 0.2 s, the nucleation and growth mechanism for the electropolymerization of aniline has been changed to a layer-by-layer mechanism. Figure 8 shows the images for the electropolymerization of aniline on HOPG at different scanning sizes. These images were obtained after a polymerization time of 0.8 s. Different layers of polyaniline are clearly seen in Fig. 8a. One can see three different polyaniline layers in Fig. 8b and Fig. 8c. The first, second and third layers appear as black, gray and white, respectively, in these images. A similar type of layer-by-layer growth can also be seen in the 2D and 3D views of Fig. 9a and Fig. 9b, respectively. These images were obtained after a polymerization time of 1.5 s. Hence, the results obtained for electropolymerization of aniline from potentiostatic current-time transient curves are comparable with the results of the AFM images at different polymerization times.

Now, it is worthwhile to compare the nucleation and growth mechanism for the electropolymerization of aniline obtained from our previous study in aqueous media with that of our present study in non-aqueous media. In our previous study, in aqueous media, the electropolymerization of aniline followed 3D progressive nucleation [25]. However, in the present work, in non-aqueous media, the electropolymerization of aniline follows

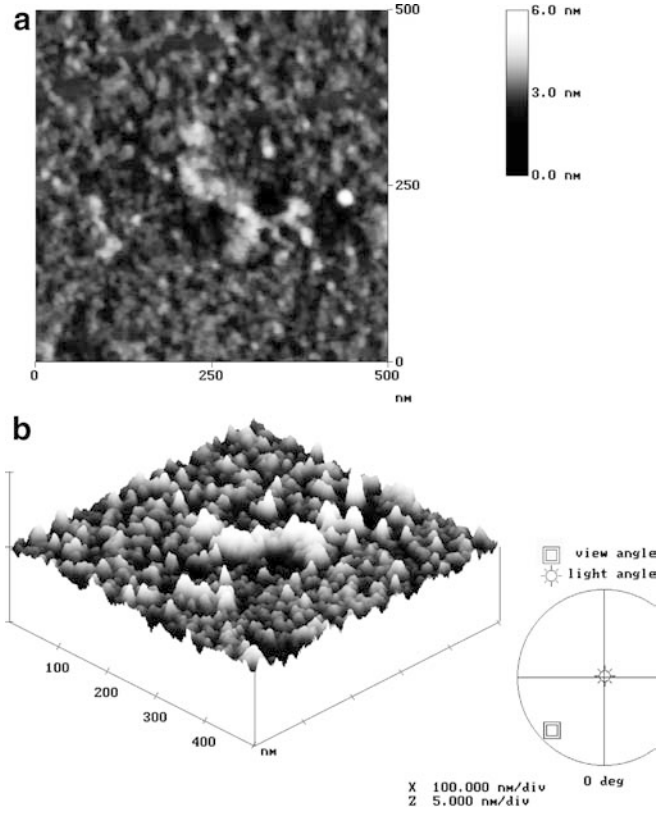

Fig. 6 AFM images of polyaniline on HOPG in 0.04 M aniline/0.06 M CF_3COOH/0.05 M $LiClO_4$ in propylene carbonate medium: (**a**) 2D view and (**b**) 3D view. Polymerization time 0.025 s; scale 500 nm

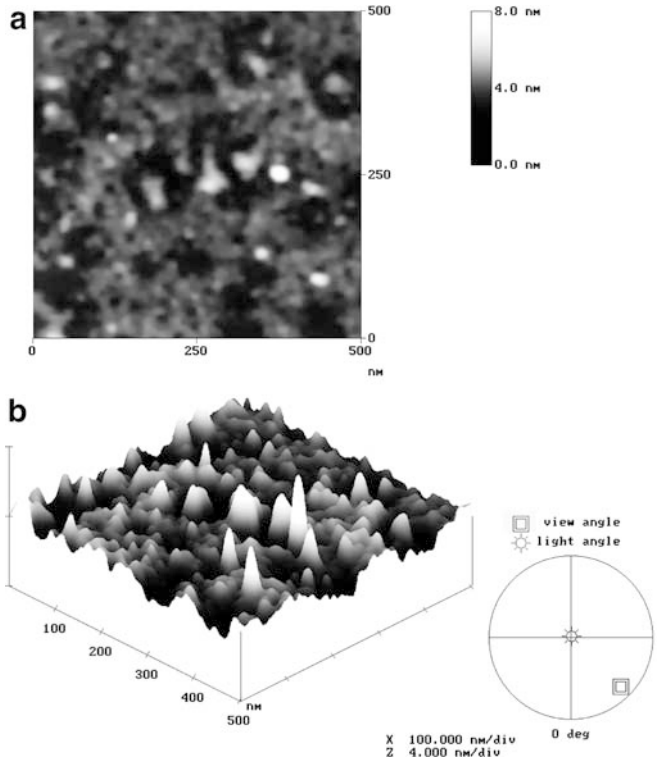

Fig. 7 AFM images of polyaniline on HOPG in 0.04 M aniline/0.06 M CF_3COOH/0.05 M $LiClO_4$ in propylene carbonate medium: (**a**) 2D view and (**b**) 3D view. Polymerization time 0.050 s; scale 500 nm

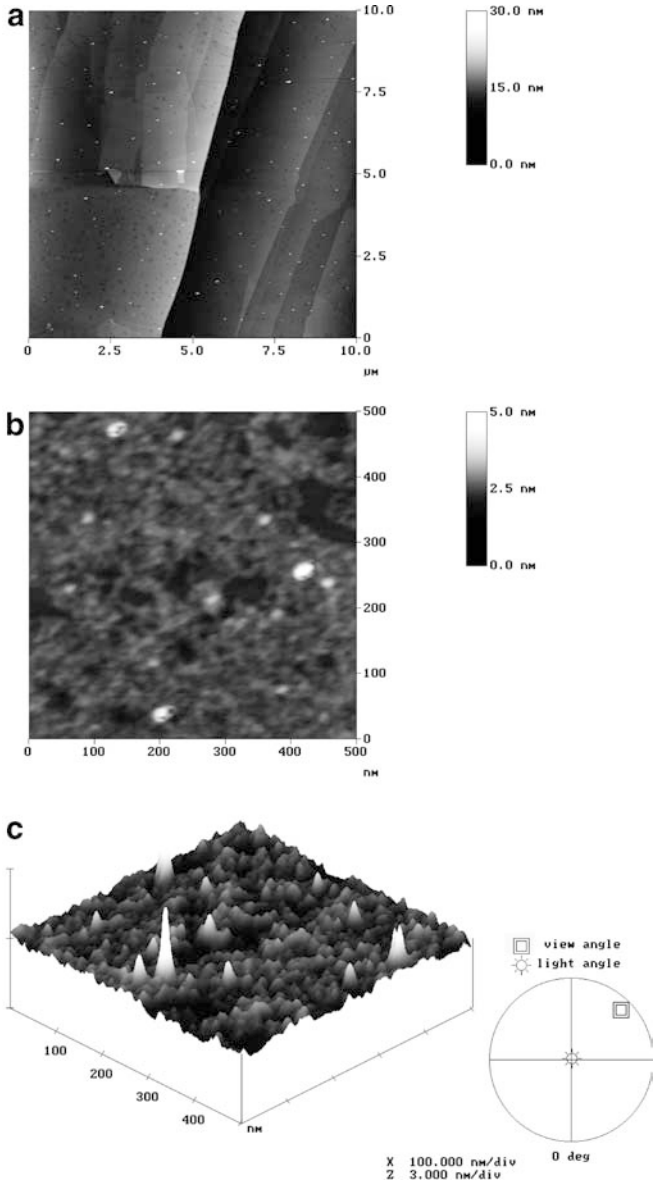

Fig. 8 AFM images of polyaniline on HOPG in 0.04 M aniline/0.06 M CF_3COOH/0.05 M $LiClO_4$ in propylene carbonate medium: (**a**) 2D view, scale 10 μm, (**b**) 2D view, scale 500 nm and (**c**) 3D view, scale 500 nm. Polymerization time 0.800 s; scale 10 μm

progressive nucleation followed by 3D growth at an early stage and layer-by-layer in the subsequent periods. This can be explained by considering the adsorption of solvent molecules on the electrode. The nucleation and growth mechanism of conducting polymers are more complex in the presence of water. In fact, the current-time transients obtained in aqueous media showed that after the double layer is charged, the current increases to reach a maximum and then drops to values near zero. Thus, the electropolymerization in aqueous media corresponds to the formation of a non-conducting or passive film. This behavior can be attributed to water molecules, which are more strongly adsorbed on the electrode than a non-aqueous solvent, and can react

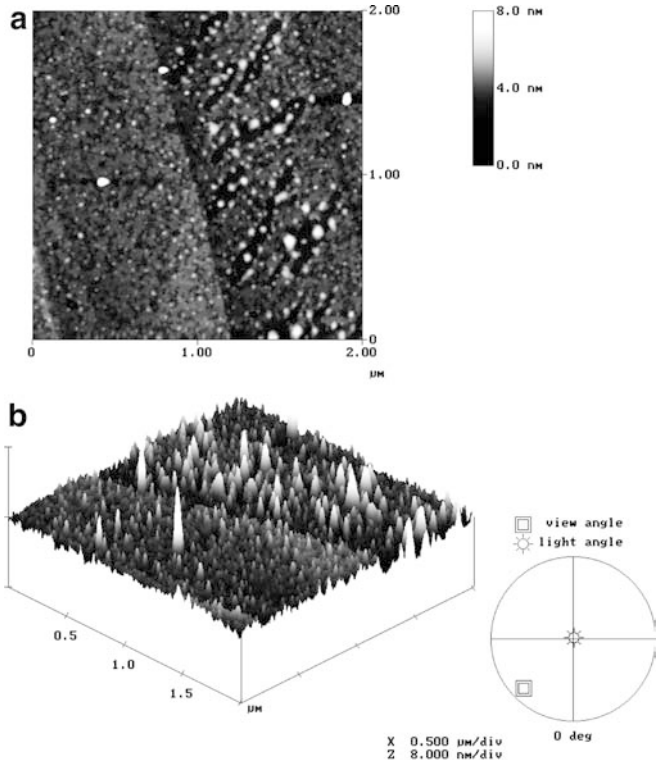

Fig. 9 AFM images of polyaniline on HOPG in 0.04 M aniline/0.06 M CF_3COOH/0.05 M $LiClO_4$ in propylene carbonate medium: (**a**) 2D view, (**b**) 3D view. Polymerization time 1.500 s; scale 2 μm

with cation radicals inhibiting the formation of conducting films [27, 28]. Hence, in the present work, we observed different types of nucleation and growth mechanism for the electropolymerization of aniline in non-aqueous media compared to the mechanism obtained in aqueous media [25].

Conclusions

The present work investigated the nucleation and growth mechanism for the electropolymerization of aniline on HOPG in propylene carbonate medium. Mechanisms were explored through the comparison of results for current-time transients with the observation of AFM images during electrochemical nucleation. It appears that the nucleation and growth involves a progressive 3D mechanism at an early stage and layer-by-layer in subsequent periods.

Acknowledgements Financial support from the National Science Council (NSC 89-2214-E-011–012 & NSC 89-TPC-7-011-008) and the National Taiwan University of Science and Technology is gratefully acknowledged.

References

1. Zotti G, Cattarin S, Comisso N (1988) J Electroanal Chem 239:387

2. Duic L, Mandic Z, Kovacicek F (1994) J Polym Sci Part A 32:105
3. Duic L, Mandic Z (1992) J Electroanal Chem 335:207
4. Fleischmann M, Thirsk HR (1963) In: Delahay P (ed) Advances in electrochemistry and electrochemical engineering, vol 3. Wiley-Interscience, New York, pp 00
5. Harrison JA, Thirsk H R (1971) In: Bard AJ (ed) Electroanalytical chemistry, vol 5. Dekker, New York, pp 00
6. Budevski EB (1983) In: Conway BE, Bockris JO'M, Yeager E, Khan SUM, White RE (eds) Comprehensive treatise on electrochemistry, vol 7. Plenum, New York, pp 00
7. De Levie R, (1984) In: Gerischer H, Tobias CW (eds) Advances in electrochemistry and electrochemical engineering, vol 13. Wiley, New York, pp 00
8. Bade K, Sakova WT, Schultze JW (1992) Electrochim Acta 37:2255
9. Mandic Z, Duic L, Kovacicek F (1997) Electrochim Acta 42:1389
10. Marcus ML, Rodroguez I, Velasco JG (1987) Electrochim Acta 32:1453
11. Miller LL, Zinger B, Zhou QX (1987) J Am Chem Soc 109:2267
12. Asavapiriyanont S, Chandler GK, Gunawardena GA, Pletcher D (1984) J Electroanal Chem 177:229
13. Hamnett A, Hillman AR (1988) J Electrochem Soc 135:2517
14. Downard AJ, Pletcher D (1986) J Electroanal Chem 206:139
15. Hillmann AR, Mallen EF (1987) J Electroanal Chem 220:351
16. Hillmann AR, Swann MJ (1988) Electrochim Acta 33:1303
17. Hillmann AR, Mallen EF (1988) J Electroanal Chem 243:403
18. Li FB, Albery WJ (1992) Langmuir 8:1645
19. Li FB, Albery WJ (1992) Electrochim Acta 37:393
20. Kontturi K, Pohjakallio M, Sundholm G, Vieil E (1995) J Electroanal Chem 384:67
21. Cai XW, Gao JS, Xie ZX, Tian ZQ, Mao BW (1998) Langmuir 14:2508
22. Hwang BJ, Santhanam R, Lin YL (2000) J Electrochem Soc 147:2252
23. Hwang BJ, Santhanam R, Lin YL (2001) Electrochim Acta 46:2843
24. Hwang BJ, Santhanam R, Wu CR, Tsai YW (2001) Electroanalysis 13:37
25. Hwang BJ, Santhanam R, Wu CR, Tsai YW (2001) J Solid State Electrochem 5:280
26. Harrison JA, Thirsk HR (1971) In: Bard AJ (ed) Electroanalytical chemistry, vol 5. Dekker, New York, pp 67, 95, 96
27. Downard AJ, Pletcher D (1986) J Electroanal Chem 206:139
28. Downard AJ, Pletcher D (1986) J Electroanal Chem 206:147